Contents list available at CBIORE journal website

International Journal of Renewable Energy Development

Journal homepage: https://ijred.cbiore.id

Research Article

Implementation of pumped hydro/photovoltaic systems in mining-degraded areas: a case study in Quadrilátero Ferrífero, Minas Gerais, Brazil

Alberto de Almeida Bossi Guimarães [a*], Adriano Silva Bastos [b], Edna Maria de Faria Viana [a], Victor Flores Mendes [c], Carlos Barreira Martinez [a,b]

[a]*Graduate Program in Mechanical Engineering - Universidade Federal de Minas Gerais (UFMG). Belo Horizonte, MG, Brasil.*

[b]*Graduate Program in Mechanical Engineering - Universidade Federal de Itajubá (UNIFEI). Itajubá, MG, Brasil.*

[c]*Department of Electrical Engineering, Hydraulic Research Center - Universidade Federal de Minas Gerais (UFMG). Belo Horizonte, MG, Brasil*

Abstract. This work presents a proposal for the transformation of mining-degraded areas into renewable energy installations, converting deactivated mine pits, in the Quadrilátero Ferrífero (QF) region in state of Minas Gerais (MG), Brazil, into reservoirs for Pumped Storage Hydropower (PSH). Additionally, it proposes the alteration of adjacent areas impacted by mining extraction process, through their conversion into Photovoltaic Power Plants (PV). This measure has the potential to turn mining liabilities into sources of energy with lower environmental impact and sustainability for society. This process allows energy to be stored in the form of hydraulic batteries, which can mitigate the effects of intermittency of photovoltaic generation in the electrical grid. The presented methodology involves mapping deactivated mines, calculating the energy potential of the coupled PSH and PV systems, and conducting an economic feasibility study for PSH implementation. The work includes a case study discussing potential local environmental impacts and the energy potentials of this solution. The case study resulted in identifying a suitable pair of mine pits for a PSH in the QF, capable of supplying the electrical grid with approximately 234.3 MW, with the generated energy cost ranging between U$112.26/MWh to U$167.22/MWh. It is concluded that utilizing inactive mines as PSH reservoirs and installing PV in adjacent mining-degraded areas are innovative and technologically feasible strategies. Economically, their implementation will depend on the market price of energy.

Keywords: Pumped Storage Hydropower (PSH), Energy Storage, Abandoned Mining Pits, Sustainable Energy, Mining-degraded areas.

Received: 8th Dec 2023; Revised: 27th March 2024; Accepted: 16th April 2024; Available online: 2nd May 2024

1. Introduction

Currently, 72% of the electrical energy consumed in the world is obtained from fossil fuels (such as oil and its derivatives) and nuclear generation (IEA, 2022). This current dependence on fossil fuels has proven to be unsustainable in the long term, since these resources are scarce and cause several environmental impacts. Therefore, it is necessary to develop the renewable energy sector to replace electricity obtained from fossil fuels in the near future.

One of the difficulties in this process concerns the fact that most renewable energy technologies are based on unpredictable natural sources, which have variable availability at different times, and therefore generate energy during time intervals that do not specifically correspond to periods of consumption (Zakeri & Syri, 2015).

A good alternative to increase the efficiency of power generating plants is to adjust the energy generated to demand. Energy storage systems align production with consumption needs as they allow the surplus energy to be captured during periods of low demand, storing it for later use when demand increases (Rehman *et al*., 2015).

In this scenario, pumped storage hydropower (PSH) stands out, which constitutes one of the most commonly used storage systems, as they offer good energy conversion efficiency, long useful life, ancillary services, quick response capacity and storage capacity on a large scale. This development consists of two reservoirs located at different heights, allowing a large percentage of the surplus electricity generated during periods of low demand to be stored. During this interval, the excess electricity is used to pump water from the lower reservoir to the upper one, thus transforming electrical energy into potential energy. Then, during periods of high demand, water is released from the upper reservoir to the lower one to generate electricity through hydraulic turbines (Vilanova *et al*., 2020).

However, PSH technology is limited by topography and land availability, as it requires a minimum elevation difference between the two reservoirs, as well as large reservoir dimensions to increase the amount of energy stored (Deane *et al.,* 2010).

One of the proposals that has been evaluated to overcome such obstacles comes from mining processes. At the end of the mining process of a mine, it is common for the site to be deactivated or abandoned. This practice is worrisome,

* Corresponding author
Email: albertoabossi@gmail.com (A.A.B. Guimarães)

considering that, in addition to providing a high maintenance cost, it can also lead to even greater environmental degradation of the area, such as soil contamination, emergence of erosion and extinction of local fauna and flora (Tonidandel, 2011).

Therefore, deactivated mining pits (DMP) have been the subject of studies to transform their status as a company liability into an asset, which is possible through their use as a reservoir for the installation of a PSH (Saigustia & Robak, 2021). This fact has the potential to minimize, or even nullify the burdens and costs associated with deactivating a mine, which, in the long term, can constitute a burden for the state and society.

In light of this, the present work aims to explore the DMP, in the Quadrilátero Ferrífero (QF) in the state of Minas Gerais (MG), Brazil, in order to use them as reservoirs for PSH, as well as the use of contiguous degraded areas from mining as space for the allocation of panels solar panels for the implementation of PVPP, investigating whether these pits, the generating power plant complex and the region in which they are located have the necessary characteristics to behave as a reservoir, and whether it is viable to its construction in terms of installed capacity.

2. Literature Review

2.1 Pumped Storage Hydropower (PSH)

PSH are large-scale energy storage systems that use electrical energy (surplus or intended for this purpose) to pump water to an upper reservoir, storing it so that, later, this water can be turbocharged, generating energy to be used, dispatched to the electrical grid.

The basic operation of a PSH, seen on Fig. 1, involves two reservoirs: an upper and a lower reservoir, connected by piping and turbine-pump and motor-generator arrangements. During periods of low electricity demand - when energy generation is greater than consumption - excess electricity is used to pump water from the lower reservoir to the upper reservoir, raising its level and storing the water's potential energy. When there is a greater demand for electricity, the water stored in the upper reservoir is released back to the lower reservoir, passing through the turbines. As the water flows, it drives turbines, generating electricity that can be delivered to the electrical grid (Görtz *et al.,* 2022). This cycle of energy storage and generation can be repeated as much as needed, making PSH an efficient way to store and supply energy at times of high demand or to compensate for fluctuations in intermittent renewable energy generation, such as wind and solar energy (Canales *et al.,* 2015).

PSH associated with a renewable power source plant, which dedicate their storage exclusively to these sources, are known as hybrid PSH. Unlike conventional PSH that primarily exchange energy with the grid, with energy from different sources, to compensate market fluctuations. Hybrid PSH emerge as a realistic and viable option to achieve high renewable energy insertion on the grid.

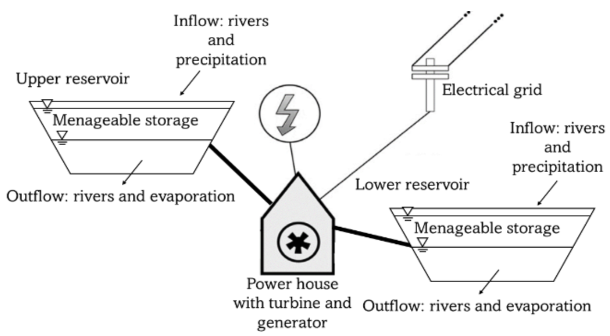

Fig. 1 - Schematic of a Pumped Storage Hydropower (adapted) (GÖRTZ *et al.,* 2022).

The main components of a PSH are: reservoirs, dams, turbine-pumps, generator-motors, control equipment, electrical substation, powerhouse and tunnels connecting the reservoirs, whether or not there may be spillways and surge tank (Brandão *et al.,* 2021).

According to the storage capacity and the height difference between the reservoirs, a PSH can have different storage cycles: hourly, daily, weekly, monthly, seasonal or multi-annual. The greater the availability of renewable and intermittent sources for storage, the shorter the generation cycle of a PSH, whether daily or weekly, for example. This is due to the fact that these sources depend on factors that are provided in short periods of time, such as sunlight in a daily period and winds in a weekly period (Nikolaos *et al.*, 2023). PSH can adopt open or closed loop configurations. In the open loop, a continuous flow of water, a river for example, is connected to the upper or lower reservoirs, with the pump turbines influencing the flow of the river, generating environmental impacts that can be mitigated by using existing dams. The closed loop is characterized by reservoirs far from continuous sources of water, reducing aquatics environmental impacts, by operating in daily or weekly cycles, being supplied at specific times by sources compensating for evaporation and infiltration (Brandão *et al.,* 2021).

Turbines that operate with a fixed speed turbines have an invariable generating and pumping capacity. On the other hand, variable speeds can be reached through an asynchronous motor-generator or synchronous motor-generator with a frequency inverter. With that, the operating range of the turbine can be expanded, and the pump capacity can be adjusted to use only the amount of energy available. at the moment (Joseph & Chelliah, 2018).

In addition to their rotation speed, there are three arrangements, divided according to their type, number, and arrangement of electrical and hydraulic machines used in PSH: binary, ternary and quaternary, where each one will have two, three, and four pieces of equipment, respectively. According to Nibbi *et al.* (2022), the most commonly used configuration is a turbopump, called reversible turbine, with fixed rotation, and a motor-generator that operate with synchronous rotation, that is a binary set.

PSH has a net energy consumption, needing more energy for pumping than they can generate, this words duo to the different price of energy during the day. They stand out in terms of emissions, surpassing fossil fuel-based thermoelectric plants. Despite concerns about reservoir-associated emissions, studies indicate that PSH have significantly lower carbon emissions than equivalent thermoelectric plants. Thus, PSH contribute not only to low-emission generation but also facilitate the integration of renewable sources, enabling emission reduction strategies in the Brazilian electrical sector (EPE, 2021; Ferreira *et al.,* 2022).

It can be considered that a PSH emerge as a possible solution with advantages arising from their low environmental impact and cost savings in their generation/storage. This approach has been widely adopted in different regions of the world, as seen in Rehman *et al.* (2015) and (Guittet *et al.,* 2016). Currently, the installed capacity of PSH in the world is 161.6 GW, which represents 94% of all electrical energy stored in the world (IHA, 2022).

In Brazil, despite the absence of a consolidated network of PSH, the growing interest and ongoing studies reflect the importance of this technology. With the national energy demand constantly rising and the increasingly significant integration of intermittent energy sources into the grid, it becomes evident that the Brazilian electrical system needs to incorporate large-scale energy storage technologies to ensure stability and operational efficiency as seen in Libanori *et al.* (2018). Studies about this technology have been carried out throughout Brazilian history. Eletrobras, in the late 80s, conducted a potential study for PSH in the South, Southeast, and Northeast regions but overlooked socio-environmental, geological/geotechnical, and hydrometeorological considerations, as revealed by EPE (2019).

In 2019, EPE presented a technical note on an inventory study for PSH in the state of Rio de Janeiro, Brazil. The aim was to map favorable locations for the implementation of these plants, and selecting the most promising locations with the characterization of the stored energy, where they defined 15 sites with great potential for a PSH. Recent studies, such as that of Hunt *et al.* (2014) propose advanced PSH models, in which there was an increase in energy storage in an annual cycle in cascade hydroelectric plants. Focusing on storing energy during the flood period in the Amazon region, it was concluded that these systems would be valid, as they require a much smaller flooded area and can achieve an efficiency close to 90%.

Internationally, in Rhodes, Greece, Arnaoutakis *et al.* (2022) discovered significant potential for PSH in conjunction with renewable sources, harnessing around 70% of the energy matrix from solar and wind sources integrated with PSH. Saigustia & Robak (2021) analyzed the potential for energy storage in abandoned mines in Poland, concluding that the technology has great potential on-site but requires detailed investigative studies for process understanding.

2.2 Photovoltaic power plant (PVPP)

Photovoltaic power plant (PVPP), or solar plant, is an installation designed to generate electricity from sunlight. It harnesses the power of the sun through photovoltaic technology, which directly converts sunlight into electricity. When sunlight shines on the solar panels, photons (particles of light) excite electrons in the semiconductor material, causing them to flow and create an electrical current. Based on sunlight, this energy source does not require inputs to operate.

Depending on their configuration, these PVPP, when installed on the ground, can be designed with fixed or variable inclination. Although variable inclination configurations can provide better energy performance, as greater use of solar incidence would be possible, this feature implies higher costs for both installation and maintenance (Gol & Ščasný, 2023).

It is also possible to place photovoltaic plates in lakes or dams; this technology structure is called Floating Photovoltaic Plant (FPVP). Such projects have a floating platform designed for the installation of photovoltaic modules. These platforms are anchored by a mooring system adjustable to fluctuations in water level, ensuring their orientation in a northerly direction. The connection of the solar panels to the substation is established using underwater cables. This option has been adopted in hybrid processes, where a Hydroelectric Power Plant (HPP) or PSH is used as a water layer for installation. According to Cazzaniga *et al.* (2019), this technology can reduce grid connection costs and water loss through evaporation. In addition to the association with water sources, there is also the possibility of associating PV with other nearby technologies, in conjunction with wind or thermoelectric plants, for example.

Several studies are found in the literature regarding hybrid generations. Margeta & Glasnovic (2010) proposed a mathematical model for sizing a PV associated with a HPP, revealing positive results. The model indicated potential implementation in cold climates with abundant solar energy, requiring a relatively small amount of water.

In a subsequent work, Margeta & Glasnovic (2012) introduced a hybrid energy system consisting of a PV combined with a PSH. This innovative hybrid plant operates continuously, using solar energy as the primary source and water for energy storage. Ma *et al.* (2015) presented a study of a PSH combined with a PV for small autonomous energy systems in remote areas. They developed mathematical models for key components, system reliability, and economic criteria, demonstrating the effectiveness of the proposed model and optimization algorithm for similar future studies.

Cazzaniga *et al.* (2019) discussed the advantages of combining floating solar panels with the 20 largest HPP globally, revealing a potential 65% increase in energy production by covering 10% of reservoirs with floating solar panels. Silvério *et al.* (2018) assessed the economic and technical viability of FPVP in HPP in the São Francisco River basin, Brazil. From an energy perspective, the HPP demonstrated an average gain of 76%, with a corresponding average increase of 17.3% in capacity factor.

Costa (2022) conducted a case study on a Brazilian HPP with FPVP on the water surface. Besides significantly reducing water evaporation, the addition of FPVP generation resulted in an average gain of 53% in energy production. The study also identified a return on the estimated investment within seven years. Silva *et al.* (2013) demonstrated the feasibility of associating technologies like batteries. In a case study, a hydrogen cell system was assessed for storing solar-generated energy in the Amazon region in Brazil, offering advantages but proving more costly than conventional battery systems.

2.3 Mining pits in the Quadrilátero Ferrífero (QF)

The history of mining activity in Minas Gerais, Brazil, which translated to English goes by “general mines”, is intrinsically linked to its own history, as evidenced by the name of the state. The Quadrilátero Ferrífero (QF), the main iron ore exploration hub in Brazil, is located in the central-southern region of Minas Gerais, Brazil, with an area of 12,785 km². With many mineral resources, including iron, manganese, gold, bauxite and precious stones, Minas Gerais, Brazil, is responsible for approximately 42% of the national production of metallic minerals (ANM, 2023).

Despite such economic relevance, the activity of mineral extraction is considered to have a high environmental impact as, in addition to being a non-renewable extractive activity, it has a high potential for environmental degradation and constitutes a possible liability for society. It is crucial to emphasize the need to establish policies and mechanisms that enable the supervision and management of impacts arising from mining activities on different segments of society. Therefore, it is imperative to implement strict environmental control and monitoring in mining projects (Fernandes & Lima, 2021).

The operation of a mine, although it brings positive economic impacts, also causes significant adverse effects on the environment, which need to be mitigated and repaired by those responsible for mining. At the end of local exploration/operation, the mining companies are assigned the work of deactivating the mines, which includes the removal of structures, the implementation of safety measures, the assessment of the impacts of deactivation on neighboring communities and the execution of social initiatives, the in order to recover degraded areas and restore the original characteristics of that environment (Fernandes & Lima, 2021).

The appropriate process for closing a mining operation plays a fundamental role in ensuring that the activity can fulfill its social function effectively. This allows economic, social and environmental benefits to be achieved for all parties involved.

Negligence at this stage can result in the creation of abandoned mines and environmental liabilities, which can have direct consequences on communities residing close to the project (FEAM, 2022). The impacts resulting from the abandonment of a mine are diverse and include the possible destruction of remaining resources, devaluation of land, lack of soil protection, land erosion and siltation of water bodies, contamination of soil and water and risks to fauna and nearby communities (Oliveira Júnior, 2001).

To ensure adequate environmental management of these projects, the specialized work of the State Environmental Foundation (FEAM) and the use of the Registry of Paralyzed and Abandoned Mines (CMPA) have played a crucial role as management instruments. The government of the state of Minas Gerais, through FEAM, formulated specific legislation for the closure of a mine – Copam Normative Deliberation nº 220/2018 (SEMAD, 2023). This resolution includes a series of guidelines that the enterprise must carry out to declare the cessation of mining activity or closure of the mine. Along with this, the body includes a Registry of Paralyzed and Abandoned Mines (CMPA) which has 520 registered enterprises.

It is important to highlight that, even with the reduction in the number of projects in a state of abandonment, FEAM continues to seek alternatives beyond inspection and application of penalties, aiming at the recovery and accountability of projects that are characterized as abandoned (FEAM, 2022). In light of this, it seen an alternative to transform these degraded places to become an economic asset, transforming these areas into a field for exploring renewable energy.

3. Method

The work proposes dimensioning a Pumped Storage Hydropower (PSH) associated with a Photovoltaic Powe Plant (PVPP), using Deactivated Mining Pits (DMP) as a reservoir. The following methodology refers to: i) definition of the pit addressed for the case study, ii) dimensioning of the PSH, including its generation potential and structural characteristics, iii) initial sizing of the PVPP, and iv) the energy available to the grid. To carry out the economic feasibility study, a sensitivity study was carried out on the costs of implementing the PSH. The cost of photovoltaic energy was determined by obtaining a value through a national auction, without calculating its implementation cost. Thus, the cost of stored energy is obtained through the PSH implementation cost, and the cost of energy generated by the combination of technologies is obtained through the cost of solar energy obtained via auction. In addition, a sensitivity analysis was conducted to define a range of generated energy costs related to the PSH implementation cost. Fig. **2** illustrates the flowchart followed by the work methodology.

The closed loop arrangement was defined for PSH as the DMP are not located in a river course. The operation takes place on a daily cycle, where during a period of the day the PSH turbines water should supply energy to the grid, and for the rest of the day it pumps water to the upper reservoir. The project must operate in such a way that the PSH supplies electrical energy to the grid during its generation period. The PVPP provides the energy necessary to pump water from the lower reservoir to the upper reservoir, and also to the grid, so that the association of PSH and PVPP sends a steady energy throughout the day to the grid. Fig. illustrates the association of the technologies in question.

3.1. Dimensioning PSH

The inventory study of a PSH is the initial part of the research. Based on a technical note developed by (EPE, 2019), this stage used part of the methodology adapted for the case study of the present work, which included the phases: mapping of promising locations for PSH implementation detailing the PSH involving its potential for generation and pumping, definition of the diameter of the pipe, tunnel and turbine.

To evaluate the site, DMP of the QF were taken into account, and a pair of suitable mining pits were selected to work as reservoirs for the PSH in question. As this arrangement configuration will be a closed cycle, there will be a need for a water source to fill the reservoirs in the initial phase, and replace water due to evaporation and infiltration losses. This source will not be defined in this work.

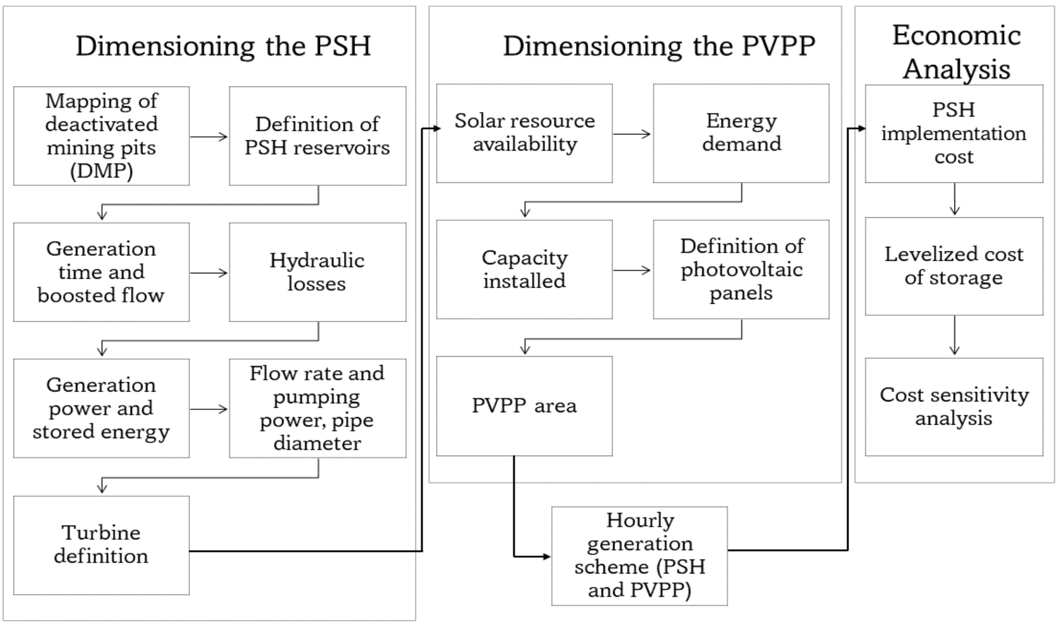

Fig. 2 - Flowchart of the methodology (author)

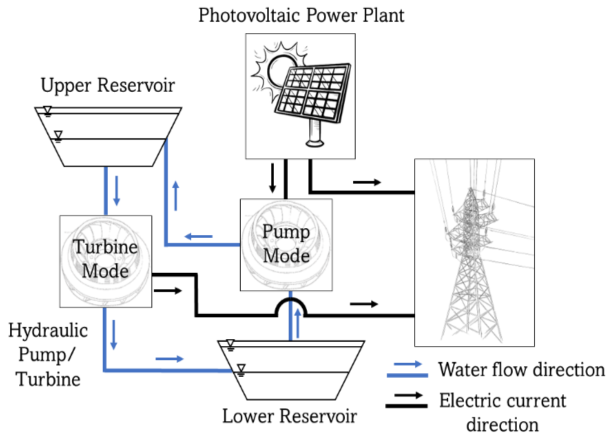

Fig. 3 - PSH and PVPP Association (author)

3.1.1. Mapping degraded mining pits

Extensive research was carried out on the DMP in the QF, taking into account the existing volumes, the geographic location, the distance and difference in level between different pits. This step was carried out through the analysis of data from the CMPA, developed by FEAM.

Through visual inspection using satellite images obtained by Google Earth ® software, registered enterprises were analyzed according to their location, their extracted mineral and their geometry in the shape of the mining pit. To work as a reservoir, the open-pit mining pit should have a basin shape, in which it would be viable (via these images) to impound a quantity of water on site, without the need for the actual construction of a dam. This characteristic can be found in iron ore mines, where extraction is voluminous and can create pits in the ground.

The ideal topographic configurations for the construction of a PSH are characterized by short horizontal distances and high vertical variations between the upper and lower reservoirs of the plant. For the maximum distance between the two reservoirs, we tried to take into account the recommendations of Barnes & Levine (2011) , which recommend that the height (gross head)/distance ratio of the pits should be at least 1/ 10. This factor may vary depending on the characteristics of the region. If there were not two nearby deactivated pits that met the aforementioned criteria, one could look for active mining pits in their proximity, prioritizing the choice that at least one reservoir was a deactivated mining pit.

3.1.2. Definition reservoir PSH

After defining the location, a mathematical model was drawn up using electronic spreadsheets in which the geographic data of the DMP were introduced to obtain the volume of the reservoir. The areas viewed via satellite were used to trace the volume of the reservoirs based on their altitude. It was sought to make the most of the available area and, through this area, create the Elevation x Area x Volume curve to identify the total volume.

The maximum and minimum heights of each reservoir were then defined. For the maximum height, the greatest height visible in satellite images that could form a reservoir inside the pit was taken into account. From this maximum height, called crest height, three meters are subtracted to obtain the maximum useful height of the reservoir.

For the minimum height, it is necessary to define a depletion height, which is the lowering of the water level in the reservoir during emptying. This height was defined for the present work as 30 m. The useful volume comprises the estimated volume between the maximum and minimum useful heights that can be pumped and turbined. The smaller useful volume of the reservoirs must be taken into account when calculating the generation potential.

The minimum height of the reservoir with the smallest useful volume is obtained through the maximum useful height minus the defined depletion. For the other, larger reservoir, the minimum height must be calculated taking into account the useful volume that will be turbined and subsequently pumped. This calculation is made using the Elevation × Area × Volume curve.

After defining the useful volume and the maximum and minimum useful heights of both reservoirs, the gross operational head were established based on Equations 1, 2 and 3:

$$Max.GD = B.max.upp - B.min.low \quad (1)$$

$$Min.GD = B.min.upp - B.max.low \quad (2)$$

$$Average.GD\ (H_b) = (Max.GD + Min.GD)\ /\ 2 \quad (3)$$

In which B is the water level in the reservoirs, maximum and minimum, upper and lower (superior and inferior)

3.1.3. Generation time and boosted flow

To determine the turbine flow based on the useful volume of the reservoir, it is necessary to define the generation time (T_g) of the PSH. The generation time refers to the time range during which the PSH is capable of generating electrical energy at its maximum power, resulting in the gradual reduction of the water level in the upper reservoir, from the normal maximum level to the normal minimum level.

For the current project, a generation time (T_g) of 14 hours was adopted. Thus, in a period of 24 hours in a day, 10 hours would be reserved for pumping time (T_b) - the time necessary to pump water from the lower reservoir to the upper one, reserved for daytime hours with greater solar incidence in the PVPP.

The turbine flow (Q_t) was calculated using an initial approximation, using the relationship between the useful volume of the reservoir and the generation time, defined according to Equation 4.

$$Q_t = V_u / T_g \quad (4)$$

In which V_u is the useful volume in [m³] and T_g generation time [h].

Fig. 3 - Percentage hydraulic loss in a hydroelectric installation as a function of gross head (Leite, 2020).

3.1.4 Hydraulic loss

The hydraulic loss, which is the decrease in pressure or energy of the water as it flows, depends on several physical factors in the pipe construction, such as joints, valves, but also diameter, roughness, flow properties, etc. One of the methods used to estimate the pressure loss of the hydraulic circuit for preliminary phases of a study is the approximation of the percentage hydraulic loss in relation to the height of the total head of the analyzed system. For this work, it will be used a graph proposed by Leite (2020), which is seen on Fig. **3**.

3.1.5 Generation Power and Stored Energy

The nominal generation power capacity is obtained by Equation 5. The stored energy ($E_{PSH.store}$) can be expressed in terms of energy stored in the upper reservoir, which is obtained by the product of the nominal generation power (P_g) and the generation time (T_g).

$$P_g = \rho * g * Q_t * H * \eta t * \eta g \tag{5}$$

In which P_g is the electrical power produced in motor generators in [W], ρ is the specific mass of water in [kg/m³], assuming an average water temperature of 25°C, g is gravity acceleration in [m/s²], Q_t is the total turbine flow in [m³/s], H is the average gross head in [m], corrected for hydraulic loss, ηt is the turbine-pump efficiency in turbine mode, adopted as a value of 90% and ηg is the efficiency of the motor-generator in generator mode, adopting a value equal to 98%.

3.1.6 Pumping power and tunnel diameter

At this stage, it is considered that the same volume of turbined water must be pumped again to the upper reservoir. Therefore, the pumping flow is calculated so that the same volume that was turbined cand be pumped in the given time. In this way, the power required for pumping (P_b) is given from Equation 6:

$$P_b = \frac{Q_b * \rho * g * (H_b + \Delta h).}{\eta b * \eta m} \tag{6}$$

As P_b is the electrical power consumed in motor generators in [W], variable with the effective lifting height, Q_b is the pumped flow in [m³/s], calculated for each effective lifting height, $H_b + \Delta h$ is the gross head in [m], which will vary between maximum gross head and minimum gross head corrected for load loss, ηb is the pump turbine efficiency in pump mode, adopted as a value of 92% and ηm is the efficiency of the motor-generator in motor mode, adopting a value equal to 98%.

The powers for the two heights in question are then calculated. The average pumping power is used to calculate the PSH efficiency. The maximum power (P_{max}) required for pumping is considered the PSH power, and is used for subsequent calculations.

The adduction/discharge tunnel is responsible for connecting the reservoirs and the powerhouse with the turbines. For the present work, a maximum water flow speed (v_e) of 4 m/s was assumed, as analyzed in the literature by (EPE, 2019; Leite, 2020). The diameter (Ø) is calculated taking into account the largest defined flow rate. As the pumping time (T_b) is shorter than the turbine time (T_g), a higher flow rate for pumping is expected. Equation 7 is used to obtain the diameter (Ø) in [m], which is defined by a relationship between the flow speed (v_e) of the water in [m/s] and the turbine flow (Q_t) in [m³/s]:

$$\emptyset = \sqrt{\frac{Q_t * 4}{v_e * \pi}} \tag{7}$$

3.1.7 Cycle Efficiency, Capacity Factor (CF) and turbine definition

The cycle efficiency (η_c) is calculated by the relationship between the electrical energy stored ($E_{PSH.store.}$) in [MWh] and the electrical energy consumed ($E_{cons.}$) in [MWh] during pumping, as per Equation 8. It is important to highlight that this value does not include losses associated with transformer performance, equipment consumption, volumetric losses, evaporation, infiltration and leaks.

$$\eta_c = \frac{P_g * T_g}{P_b * T_b} = \frac{E_{PSH.store.}}{E_{cons.}} \tag{8}$$

Capacity Factor (CF) is a measure that expresses the relationship between the actual amount of electricity produced during a given period and the maximum amount theoretically generated if the plant operated continuously during that period. In other words, it tells us how effectively a plant is operating relative to its maximum power generation potential. The CF is expressed by Equation 9:

$$FC = \frac{E_{prod}/\Delta t}{P_{max}} \tag{9}$$

In which, E_{prod} is the energy generated in [MWh] in the period considered, P_{max} is the installed power in [MW] and Δt is the time considered.

To define the equipment, knowledge developed by Schreiber (1978) was taken into account. The most primitive solution of choice would be the installation of a generating unit composed of a turbine and a generator, and a pump and a motor, that is, a quaternary set. However, this configuration, although it can provide more appropriate parameters and shorter start-up times specific to the project in which it was developed, is expensive and therefore not widely used.

Thus, a binary set was adopted, with the installation of a turbine and a pump defined as proposed by Schreiber (1978), in which he indicates the relationship between the plant's gross head and specific speed of the main types of turbines. reversible. The specific speed (n_s) is defined as the rotational speed of a turbine. The number of turbines was defined through the installed power of the reversible unit using sets with power of approximately 50, 100, 150 and 250 MW.

3.2 PVPP needed

In this study, a ground-mounted PVPP was chosen, aiming to potentially utilize degraded mining areas adjacent to the defined DMP as the study's focal point. The analysis of the available solar resource, the energy demand and the sizing of the photovoltaic plant in terms of area and power are presented below.

3.2.1. Solar Resource Available

The data of the solar irradiation comes from the SunData tool from (CRESESB, 2018), which calculates the average daily solar irradiation, in the monthly period, at any point in the Brazilian territory. The use of the month with the lowest solar irradiation must be taken into account when calculating the installed capacity of the PVPP. This method assumes that, if the system works properly this month, the same should occur in the remaining months of the year, producing more energy when conditions are more favorable.

The energy demand, or daily required energy (E_{PVPP}), is a value given in [MWh] necessary for sizing the PVPP. This value is obtained through Equation 10, where the pumping time (T_b) is multiplied by the PSH generation power (P_g), which will be supplied firmly to the network, and by the average pumping power required (P_b).

$$E_{PVPP} = T_b * (P_g + P_b) \quad (10)$$

The installed capacity of a PVPP is given in Watt-peak (Wp). As the power of a photovoltaic panel varies depending on irradiation and temperature, Wp was established as the power of the panel in Standard Test Conditions (STC), which considers an irradiation of 1000 W/m² and the temperature of the 25°C photovoltaic cell. This capacity can be calculated based on the energy demand (E_{PVPP}), daily solar availability (HSP) and PVPP efficiency. This is done according to Equation 11.

$$W_{plant} = \frac{E_{PVPP}}{HSP * \eta_{PVPP}} \quad (11)$$

In which W_{plant} is the nominal power of the plant in [Wp], HSP is the Peak Sun Hours in [kWh/m²] and η_{PVPP} is the efficiency of the PVPP. It will be adopted in this work the average efficiency equal to 77%

The number of photovoltaic panels ($N°_{panels}$) is calculated according to Equation 12, in a simple calculation of the defined installed power [W] of the PVPP and W_{panel} is the nominal power [W] of each photovoltaic panel:

$$N°_{panels} = \frac{W_{plant}}{W_{panel}} \quad (12)$$

The area required for installing the photovoltaic plant is defined by the sum of the area of each panel plus a percentage of free area intended for access by machines and technicians responsible for maintenance, cleaning and assembly of the system. It is also important to highlight that there is a minimum distance between the photovoltaic modules, preventing possible shadowing of the solar panels on each other. For the present work, an approximation was made of the values obtained from a significant PVPP in Brazil, the Janaúba Solar Complex. Located in Minas Gerais, the plant holds the title of the largest photovoltaic plant in Brazil. Taking into account the total number of panels and the area occupied by the solar park, a reference value equivalent to 717 solar modules per hectare was obtained, using panels whose modules add up to 550 Wp each, according to data obtained from Elera Renováveis (2023). This reference value allows us to approximate the area used, accounting for panels, inverters, structures and the like.

Once the total area required by the plant is obtained, an area adjacent to the mines chosen for allocation of the panels must be chosen. This area must include, as a priority, abandoned or deactivated mines and flat areas, without the shape of a pit. If there are no deactivated mining areas nearby, it is suggested to evaluate mines in operation, and, as a last resort, areas without construction and with flat/favorable geometry.

3.3 Daily generation scheme

With the PSH and PVPP installations defined, a daily generation scheme is then developed for the enterprise by allocating energy throughout the day. In it, the source and destination of the energy generated and consumed are simulated, hourly, in a daily period.

The calculation of energy generation and its hourly allocation is carried out to provide a basis for the possible self-sufficiency of the installation. It takes into account the electrical energy production potential of PSH and PVPP installations, over a period of one day, at hourly intervals. This simulation is carried out using data provided by the SAM – System Advisor Model software, developed by the National Renewable Energy Laboratory.

Initially, an average daily solar irradiation curve at the defined location is considered. The incident irradiation at the defined location is provided in W/m², and allows hourly solar generation to be calculated through the integral of the graph area, at defined intervals. The average daily irradiation curve of the month with the lowest incident solar irradiation must then be used. For comparison purposes, the same procedure is performed with a higher incident irradiation, in a month with a high irradiation rate.

3.4 Economic feasibility study

The economic feasibility study is carried out in two parts. First, the implementation cost of the PSH will be calculated, and then, through the calculation of the levelized cost of storage (LCOS), the cost of final energy is calculated. This leveling takes into account the payback period for the investment to pay off, thus providing data to guide the venture investor. The useful life of the PSH, investment, maintenance and operation costs must be taken into account, thus obtaining the value of the energy cost. This step is carried out using part of the model developed by Stocks *et al.* (2021).

The final cost, called cost per unit of energy generated, is derived from international methodologies and imposed measures adopted for this particular study. In this way, a cost sensitivity analysis is conducted, exploring different implementation cost projections and the corresponding costs associated with the energy generated.

3.4.1 Capital Costs (Capex)

The capital cost of a closed-cycle PSH can be roughly divided into capital costs associated with energy generation and those associated with the capital cost of energy storage. The capital costs associated with power generation include water transportation, powerhouse, pump/turbine, generator and substation. The capital costs associated with energy storage comprise the cost of reservoirs.

The model developed by Stocks *et al.* (2021), relied on hydraulic engineering consultants using detailed spatial analysis of a variety of locations. Costs are reported in US dollars. This was used to calculate the implementation capital.

The main cost of building reservoirs is moving rocks to form a dam. Considering that deactivated mining pits (DMP) were objects of choice, aiming at their characteristic as a pit format to minimize costs associated with the construction of reservoirs, a low cost is expected compared to other projects. This, called the cost of the storage component ($C_{arm.}$), was defined based on the volume of a dam around the entire pit (upper and lower) and an average construction cost (Y), being the same used by Stocks *et al.* (2021). The defined cross-section of the dam is made up of a trapezoid with a lower base of 4 m, an upper base of 3 m and a height of 2 m, which must be built around the entire perimeter of both reservoirs. Equation 13 demonstrates the cost of the storage component ($C_{resv.}$).

$$C_{resv.} = Y * A_{dam} * (PR_{upp} + PR_{low}) \quad (13)$$

In which, Y is the defined cost of 168 in [$/m³], PR_{upp} is the perimeter in [m] of the upper reservoir, PR_{low} is the perimeter in [m] of the lower reservoir, and A_{dam} is the area in [m²] of the cross-section of the dam.

The relationships for power generation costs comprise two components: tunnel and powerhouse. These have a complex relationship with the characteristics of the location. It is assumed that the tunnel, responsible for transporting water between the reservoirs, is composed of a vertical well, the cost of which is proportional to the power of the PSH, P_{max} in [MW], the horizontal distance between the reservoirs, S in [m], and the height H_b in [m], as demonstrated in Equation 14.

$$C_{tunnel} = (66.000 * P + 17.000.000) + S * (1.280 * P_{max} + 210.000) * H_b^{-0,54} \quad (14)$$

The cost of the powerhouse includes civil, mechanical and electrical costs. It is assumed that the engine room is excavated. Civil costs include excavation of the machine and transformer rooms, and tunnels for vehicular access and electrical access. Mechanical includes pumps/turbines and electrical generators, including commissioning. Equation 15 represents the cost of the engine room, where H_b in [m] is the height of the project and P_{max} in [MW] the power.

$$C_{p.house} = 63.500.000 * H_b^{-0,5} * P_{max}^{0,75} \quad (15)$$

The capital cost, called C_{Capex}, is the sum of the reservoir, tunnel and powerhouse costs. The cost of the land was not taken into account.

3.4.2 Levelized Cost for Electrical Storage (LCOS)

To obtain the levelized cost, it is necessary to calculate the Capital Recovery Factor (FRC). It refers to the rate used to calculate the periodic amount needed to recover the initial investment over a period of time. This concept is often used in cost analysis, especially in investment projects. The FRC takes into account the initial cost of the investment, the desired recovery period and the associated interest rate. Equation 16 expresses how FRC can be calculated.

$$FRC = \frac{(1+i)^n * i}{(1+i)^n - 1} \quad (16)$$

In which i is the interest rate adopted for the project and n is the useful life of the project, in this case considered in years.

The FRC is used to calculate the annual Capex cost ($C_{Annual.Capex}$) according to Equation 17.

$$C_{Annual.Capex} = C_{Capex} * FRC \quad (17)$$

The maintenance and operation cost ($C_{O\&M}$) is adopted as 5% of the Capex capital cost, per year. Thus, the annual cost of PSH ($C_{Anual.PSH}$) can be obtained, according to Equation 18.

$$C_{Annual.\mathrm{PSH}} = C_{Annual.Capex} + C_{O\&M} \quad (18)$$

The cost for storage is obtained according to Equation 19, with energy produced annually with an availability of 95% ($E_{Annual.95}$).

$$C_{Energy.Store.} = \frac{C_{Annual.UHR}}{E_{Annual.95}} \quad (19)$$

Finally, the generated energy cost is obtained, which takes into account the cost of stored energy and the cost of available solar energy. To this end, the cost of solar energy supplied through the 2022 A-5 New Energy Auction (EPE, 2022) was taken into account. In it, it is possible to find the winner of the auction for the supply of energy from PVPP, where the average price of R$ 171,51 /MWh is obtained, being ($C_{Energy.Solar}$). The value is then converted to dollars, adopting a quote for November/2023, with R$4.90 being the value of U$1.00. Equation 20 finally shows the cost of energy generated for the adopted project.

$$GEC = C_{Energy.store.} + C_{Energy.Solar} \quad (20)$$

3.4.3. Cost sensitivity analysis

Cost sensitivity analysis explores different cost and deployment projections, providing different costs of generated energy, thus creating a margin. This approach is crucial for evaluating project viability in varying scenarios, allowing for strategic adaptation in the face of fluctuations in initial installation costs.

Within the scope of this study, changes in the implementation cost were considered, representing 70%, 80%, 90%, 110% and 120% of the installation capital cost (Capex). Operation and maintenance costs remained constant. To define the cost of available solar energy supplied, the value of the previous year's auction, New Energy Auction A-5 De 2021 (EPE, 2021a) was evaluated, with the average cost being R$ 166.90/MWh. In view of the fluctuation in value in auctions, representations of 70%, 80%, 90%, 110% and 120% of the cost of the solar energy supplied were made.

A detailed table was created to present the values obtained in each of these configurations, providing a comprehensive view of the variations in costs associated with the energy generated.

4. Results and discussion

4.1 Identification or reservoir PSH

Using Google Earth® software, the area comprising the Iron Quadrangle (QF) was plotted, according to the coordinates of the Geological Map of the Iron Quadrangle version 2020 (QFE2050, 2019). Its ends are located at coordinates between 19°30' and 20°43'South and 43°07' and 44°30' West. In Fig. 4 it is possible to see the delimitation of the QF on the map.

Of these 34 mines, 29 do not have suitable geometry to be used as a reservoir for the PSH and therefore were not considered in this study. Analyzing the favorable developments, the height (gross head)/distance ratio between the possible pairs of pits to be defined was calculated. No pair of deactivated

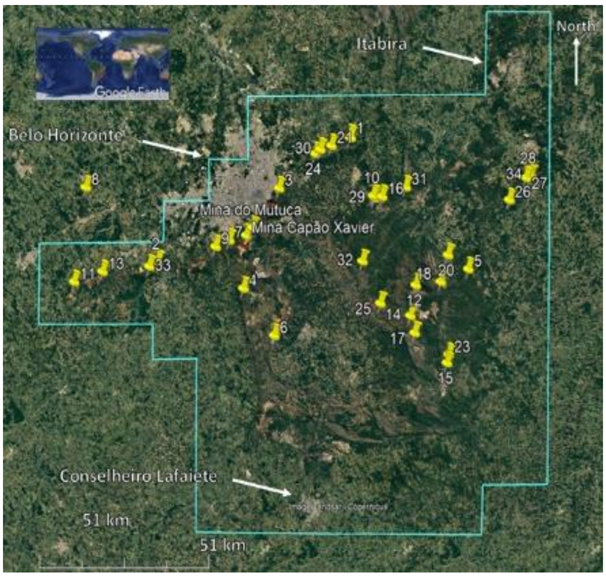

Fig. 4 - Map of Quadrilátero Ferrífero with FEAM mines (Google Earth - Image Landsat 2023).

Table 1
Enterprises quoted for the project

Name	City	Situation	Reservoir Area	Elevation on H.max	Perimeter
Geral do Brasil Mining	Brumadinho	Paralyzed	11,786 m²	1,340 m	472 m
Córrego do Meio Mine	Sabará	Paralyzed	28,000 m²	950 m	628 m
Viga Norte Mine	Nova Lima	Paralyzed	33,785 m²	1,430 m	687 m
Capanema Mine	Itabirito	Paralyzed	178,489 m²	1,440 m	2,206 m
Mutuca Mine	Nova Lima	Paralyzed	467,939 m²	1,220 m	2,826 m
Mar Azul Mine	Nova Lima	Active	139,983 m²	1,150 m	1,445 m
Pico Mine	Itabirito	Active	250,175 m²	1,345 m	2,186 m
Tamanduá Mine	Nova Lima	Active	384,427 m²	1,170 m	2,668 m
Águas Claras Mine	Belo Horizonte	Active	513,311 m²	1,060 m	2,747 m
de Pau Branco Mine	Nova Lima	Active	581,662 m²	1,420 m	3,610 m
Horizontes Mine	Nova Lima	Active	648,300 m²	1,330 m	3,814 m
Capão Xavier Mine	Nova Lima	Active	806,750 m²	1,330 m	3,657 m

Source: author

pits was found that satisfied the ratio greater than 0.1 between these projects. Therefore, it was looked for active mining sites that were not included in the CMPA registry, but that best fit the project criteria.

Five paralyzed favorable developments were found in the CMPA registry, then, active pits that could work as a reservoir were researched. Table 1 includes the relevant active projects and deactivated projects considered for the project, as well as height data (verified via satellite image topography) and area at the highest height verified for water depth.

According to the projects listed on Table 1, we have the following considerations: the Geral mines do Brasil Mining (Brumadinho), Córrego do Meio Mine (Sabará), Capanema Mine (Itabirito), Águas Claras Mine (Belo Horizonte) and Pico Mine (Itabirito) do not have another pit close to the site, verified within a radius of 3km, being considered unfeasible for the present study.

The Horizontes Mine is located 2,820 m from the Tamanduá Mine, the height/distance ratio between both mines is 0.057. Both projects are active, which undermines the central idea of the work of using degraded areas. It must also be considered that they are separated by a residential condominium (Morro do Chapéu). In this case, the penstock that would connect both reservoirs would necessarily pass under the condominium, making it difficult for government agencies to approve the project, since the private property located on the surface has a high number of residences. Therefore, they were discarded as hypotheses for the work.

Mutuca Mine and Viga Norte Mine are paralyzed projects that can be quoted for the present study. Both of them have nearby mine pits currently active, with a high degree of exploration of the site. The Pau Branco Mine, located 1,270 m from the Viga Norte Mine, could act as an upper reservoir. The Capão Xavier Mine is located 1,978 m from the Mutuca Mine, and can act as the project's upper reservoir. The pairs and their height/distance relationships can be seen in Table 2.

Fig. 5 – Mutuca Mine and Capão Xavier Enterprise (Google Earth - Image Landsat 2023).

In light of this, it is analyzed the gross head height/distance coefficient, as recommended by Barnes & Levine (2011). Since the closest coefficient to 0.1 is the one of the pair Mutuca Mine and Capão Xavier Mine, it was decided that the present work would be carried out using these two enterprises.

In Fig. 5, it is possible to see the isometric view via satellite of the chosen project, with demarcation of the reservoirs and penstock, which is the shortest distance between the two reservoirs. The coordinates of Mutuca Mine are 20°01'42.7"South and 43°57'44.9"West.

4.2 PSH Technology

Once the mining pits were defined, data relating to the elevation, area and volume of the reservoirs were obtained to draw the Elevation × Area × Volume curves. This was obtained from the approximation of the area varying with each meter of

Table 2
Pairs of pits quoted for the case study (author)

Upper Reservoir	Lower Reservoir	Distance	Gross head	Height/distance
Capão Xavier Mine	Mutuca Mine	1.978 m	116.5 m	0.056
Mutuca Mine	Mar Azul Mine	2.768 m	70 m	0.025
Viga Norte Mine	Pau Branco Mine	1.270 m	10 m	0.008

Source: author

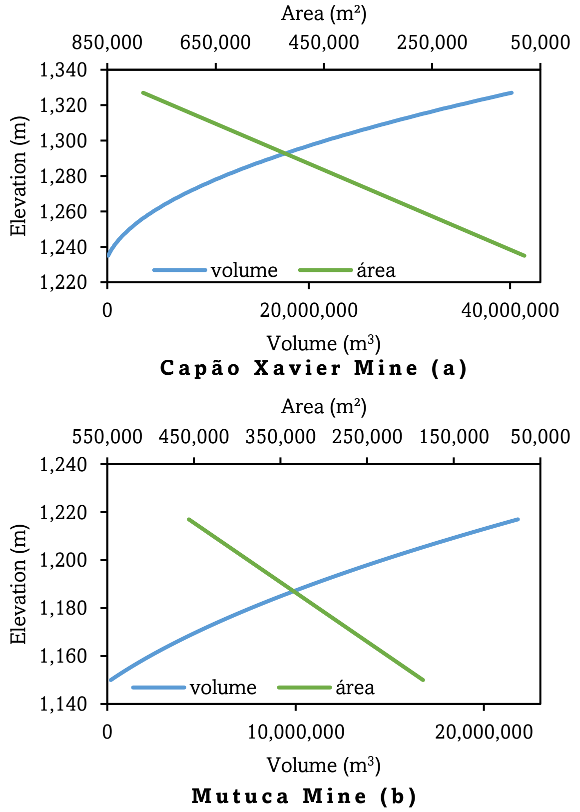

Fig. 6 - Graphic elevation x area x volume of the upper reservoir - Capão Xavier Mine (a), graphic elevation x area x volume of the lower reservoir – Mutuca Mine (b) (author)

height in elevation. Fig. 6 illustrate these curves for the reservoirs.

By depleting 30 m, the useful volumes in both reservoirs were calculated. The volume of the Capão Xavier Mine (upper) is 20,183,713 m³, while that of the Mutuca Mine (lower) is equivalent to 12,254,659 m³. Therefore, the volume of the Mutuca Mine is considered as the useful volume of the project. It is important to highlight that a new depletion was calculated for the upper reservoir (Capão Xavier Mine) based on the defined useful volume.

The evaluation of gross head, a key aspect in assessing the site's hydraulic potential, is calculated derived using Equations 1, 2, and 3. The range of gross head values are: from a maximum ($Max.GD$) of 140 meters to a minimum ($Min.GD$) of 93 meters, with an average ($Average.GD$) of 116.5 meters. This detailed analysis helps us understand the terrain's variation and how it affects our options for harnessing hydraulic energy.

Using the data in Table 5, it is possible to calculate the flow/power of the installation that can be installed in this location. The values presented in this table were obtained from the elevation x area x volume graphic developed for both reservoirs. These values facilitate an examination of the installation's capabilities in terms of flow and power. Thus, the turbine flow (Q_t) calculated by Equation 4, using the generation time (T_g) of 14 h is 243.15 m³/s.

The incorporation of hydraulic loss percentages, as elucidated in Leite (2020), adds an additional layer of precision to the assessment. The establishment of a 4.1% hydraulic loss, calibrated against the defined average gross head of 116.5 meters, adjusted the average gross head to 111.72 meters. This adjustment reflects the effort to obtain a more accurate result.

Table 5
Reservoir Data

	Lower Reservoir - Mutuca Mine	**Upper Reservoir - Capão Xavier Mine**
Elevation min.	1,150 m	1,235 m
Elevation max. (crest)	1,220 m	1,330 m
Elevation max. useful	1,217 m	1,327 m
Depletion	30 m	17 m
Elevation min. useful	1,187 m	1,310 m
Reservoir Height	67 m	92 m
Total Volume	21,805,337 m³	40,144,682 m³
Useful Volume (V_u)	12,254,659 m³	12,283,296 m³

Source: author

Equation 5 is used to compute the generation power, using data from Table 3, giving us a tangible measure of the installation's potential output. With a substantial 3,279.8 MWh of stored energy ($E_{PSH.store}$), as outlined in the table, we have a solid foundation for assessing feasibility.

For a day, 14 hours are allocated to generation via turbine and 10 hours to pumping. In this case, the pumping flow is 1.4 times the turbine flow. According to Equation 6, the powers required during the pumping operation were then calculated, according to the maximum and minimum heights, both corrected for the pressure loss in question. Table 4 shows the values used in Equation 6 and the pumping power. From the average pumping power required, we have the pumping energy consumed ($E_{cons.}$) in the amount of 4,124.4 MWh. The cycle

Table 3
Generation Power

Average head (H)	111.72 m
Turbine efficiency (ηt)	90 %
Generator efficiency (ηg)	98 %
Specific mass of water at 25° (ρ)	997 kg/m³
Gravity (g)	9.807 m/s²
Turbine flow (Q_t)	243.15 m³/s
Electric power of generation (P_g)	234.3 MW

Source: author

Table 4
Pumping Power

Pumped flow (Q_b)	340.41 m³/s
Max. Height.	134.26 m
Min. Height	89.19 m
Pump efficiency (ηb)	92%
Motor efficiency (ηm)	98%
Power Required H.max. (P_{max})	495.64 MW
Power Required H.min.	329.24 MW
Average Power Required	412.44 MW

Source: author

efficiency, calculated from Equation 8, is then equivalent to 79.52%.

Considering the highest flow rate, which is the pumping flow, to calculate the tunnel diameter, using Equation 7, we have a pipe with a diameter (Ø) of 10.41 m. As this was an initial analysis, a configuration with four tunnels was adopted, reducing the diameter value when compared to just one unit. Therefore, four tunnels with a diameter (Ø) of 5.20 m were adopted for the installation.

The power of the PSH is defined by the highest power required for pumping (P_{max}). Therefore, the installation's power is equivalent to 495.64 MW. This value is different from the project's generation power, which, according to 14 h in a day, is 234.3 MW.

According to item 3.1.7, the installation will be equipped with binary sets, consisting of four Francis-type turbine/pump units, radial-axial flow of 123.90 MW (the installation power being divided by four) each, with speed specific speed of approximately 190 rpm. The turbine power must be equal to the highest power demanded by the system, which is the pumping condition at its maximum height, that is, when the upper reservoir is close to its maximum capacity and the lower one is close to its minimum.

The capacity factor (FC), according to Equation 9, is calculated considering the time interval of one day (24h), being equivalent to 27.57%.

4.3 PV Technology

For the defined location, the average solar irradiation was sought on a surface inclined at 20°, provided by CRESESB (2018). According to the data, it was identified that the month with the lowest irradiation is November, which is consider for subsequent calculations the value of 4,77 kWh/m²/day.

The daily energy demand (E_{PVPP}), calculated using Equation 10, is equivalent to 6,467.1 MWh. The installed capacity of the PVPP was calculated according to Equation 11, the values for the calculations are shown in Table 6. Based on Equation 12, around 3.20 million panels would be needed, considering generic monocrystalline panels with 550 Wp of power. The total area occupied would be approximately 4,493 ha, considering the area of the panels plus the area required for distancing, inverters, natural ventilation and maintenance. This value is an approximation of the Janaúba Solar Complex.

To allocate the necessary area, degraded areas adjacent to the mines in question and degraded areas of mines close to the project were taken into consideration. Therefore, the degraded areas of nearby mines could be used to allocate the panels and equipment necessary for the PVPP. The adjacent areas, evaluated via satellite image, for each mine are: Mutuca Mine with 277 ha, Tamanduá Mine with 115 ha, Horizontes Mine with 253, Pico Mine with 632 ha and Sapecado Mine with 684 ha. These have a total area of 1,961 ha, requiring an additional 2,504 ha to allocate the panels that make up the PVPP. These areas can come from mining land or private land.

It is important to highlight that these areas were selected via satellite images, avoiding pit areas. As this is an idea in its initial phase, it is suggested for future work that the parameters of the areas, such as the slope of the terrain and real availability, be better analyzed.

Table 6
PVPP Power Installed

Energy demand (E_{PVPP})	6,467.1 MWh
HSP	4.77 kWh/m²
PVPP efficiency (η_{PVPP})	77.0%
PVPP Power (W_{plant})	1,760.76 MWp

Source: author

4.4. Daily generation scheme

The calculation of energy generation and its hourly allocation is initially carried out using the average daily hourly irradiation curve for the month of November, which has the lowest average daily solar irradiation. Through the integral of the curve, it is possible to obtain the hourly generation of electrical energy for 1000 Wh/m², which when multiplied by the power of the PVPP installation, provides the amount of electrical energy produced for the time of day. The same was also carried out for the average daily hourly irradiation curve for August, the month with the highest average, in order to evaluate a day with a high incidence of irradiation.

The curves referring to the average daily irradiation in a given month were obtained using the SAM software (System Advisor Model (SAM), 2023), in a location close to the mines, whose geographic coordinates are 19°51' South and 43°57' West. Fig. 7 illustrate both curves for the months of November and August. Using these curves, the energy generated in both cases in different months was calculated to evaluate the energy produced by PVPP. A generation/pumping scheme is then drawn up, illustrated in Table 7. The analysis of this table is carried out below. Losses associated with technologies are not considered in the Table, as the value is embedded in the efficiency of each installation.

The first column [1] illustrates the hours of the day. In the second [2] and third column [3], the powers injected into the grid by PSH (turbine generation) and PVPP (solar generation) are shown, respectively. The sum of the two powers for each hour of the day is seen in the fourth column [4]. The required pumping power, seen in column five [5], is the power necessary for the PVPP to pump water from the lower reservoir to the upper one. This power in the first hour corresponds to the lowest power required, obtained in Equation 6, in which the lowest height is taken into account, since the lower reservoir is full and the upper one is empty (in relation to its useful volume). Column six [6] corresponds to the sum of the power injected into the network by the PVPP [3] and the required pumping power [5].

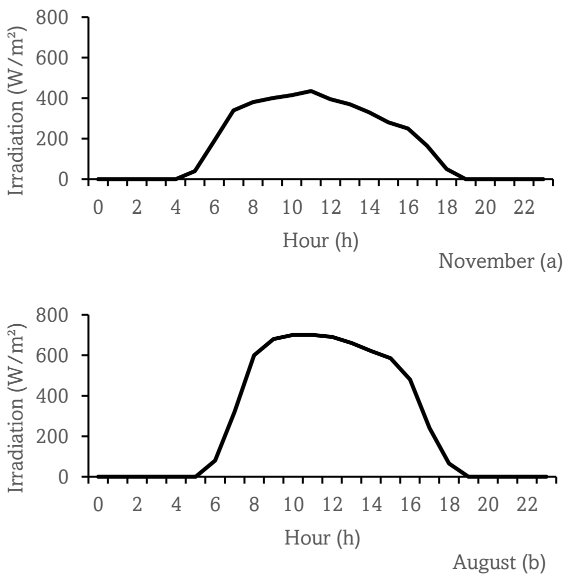

Fig. 7 - Average daily solar irradiation for the month of November (a) and August (b) (Software SAM – adapted)

Table 7
Generation/Pumping Scheme

Time on a day [h] [1]	Power injected into the grid by PSH [MW] [2]	Solar power injected into the grid [MW] [3]	Power supplied to the grid [MW] [2]+[3]= [4]	Power required for pumping [MW] [5]	Total Power Required by the Solar Plant [MW] [6]	Hourly Solar Energy Available Month November [MWh] [7]	Hourly Solar Energy Available Month August [MWh] [8]
1	234.27	0.00	234.27	0.00	0.00	0,00	0,00
2	234.27	0.00	234.27	0.00	0.00	0,00	0,00
3	234.27	0.00	234.27	0.00	0.00	0,00	0,00
4	234.27	0.00	234.27	0.00	0.00	35,22	0,00
5	234.27	0.00	234.27	0.00	0.00	202,49	0,00
6	234.27	0.00	234.27	0.00	0.00	466,60	70,43
7	0.00	234.27	234.27	329.24	563.51	633,87	352,15
8	0.00	234.27	234.27	347.73	582.00	686,70	809,95
9	0.00	234.27	234.27	366.22	600.49	717,51	1.126,89
10	0.00	234.27	234.27	384.71	618.98	748,32	1.214,92
11	0.00	234.27	234.27	403.20	637.47	730,71	1.232,53
12	0.00	234.27	234.27	421.68	655.95	673,49	1.223,73
13	0.00	234.27	234.27	440.17	674.44	616,27	1.188,51
14	0.00	234.27	234.27	458.66	692.93	537,03	1.126,89
15	0.00	234.27	234.27	477.15	711.42	466,60	1.060,86
16	0.00	234.27	234.27	495.64	729.91	365,36	937,60
17	234.27	0.00	234.27	0.00	0.00	189,28	633,87
18	234.27	0.00	234.27	0.00	0.00	44,02	268,52
19	234.27	0.00	234.27	0.00	0.00	0,00	57,22
20	234.27	0.00	234.27	0.00	0.00	0,00	0,00
21	234.27	0.00	234.27	0.00	0.00	0,00	0,00
22	234.27	0.00	234.27	0.00	0.00	0,00	0,00
23	234.27	0.00	234.27	0.00	0.00	0,00	0,00
24	234.27	0.00	234.27	0.00	0.00	0,00	0,00
Total	3279.77	2342.69	5622.46	4124.40	6467.09	7113,47	11304,07

Source: author

The seventh column [7] is responsible for the available solar energy generated by the PVPP. This column was constructed taking into account the average daily hourly irradiation curve for the month of November. The eighth column [8] represents the available solar energy generated by the PVPP in a condition where irradiation is much higher than in the month of November, which takes into account the average daily hourly irradiation curve for the month of August, which represents the highest annual average.

It is possible to verify that the total power required by the PVPP does not always correspond to the energy available from solar generation. For the condition with low solar irradiation, on one day in November, it is seen that there is not enough energy for pumping from 13:00 until 16:59. The same occurs on an August day with high solar incidence, but for the hours of 7:00 am to 7:59 am.

It should be noted that on rainy days, irradiation may be minimal, while on sunny days, irradiation may be maximum. Rainy days can also fill the upper reservoir depending on rainfall, but calculations regarding this balance must be performed to make statements about the current project. One solution to this issue adopted for this work is to complement the energy required during these times with grid energy, also adopting the cost of energy from national auctions.

4.5. Economic feasibility study

The initial phase of our financial analysis delved into computing the Capex capital cost, an important determinant of project viability. This intricate process involved a breakdown of expenses, encompassing storage, tunnel, and powerhouse costs. Notably, the powerhouse cost was crafted to accommodate four turbines, ensuring a robust infrastructure to harness hydroelectric potential. The dataset presented in Table 8 provided the necessary inputs for calculating storage costs, meticulously executed through Equations 13, 14, and 15.

The methodology followed a systematic approach, commencing with the calculation of the FRC using Equation 16, with due consideration to an interest rate of 10% and a projected useful life of 30 years for the PSH. Leveraging Equation 17, it was derived the annual capital cost, a cornerstone in the financial evaluation. An allocation of 5% of

Table 8
Data for calculating Capex capital cost

Cost Y		168.00 U$/m³
Dam area (A_{dam})		7.00 m²
Upper reservoir perimeter ($PRupp_{upp}$)		3.653.0 m
Lower reservoir perimeter (PR_{low})		2.826.0 m
Horizontal distance between reservoir (S)		1.978.0 m
Storage cost ($C_{resv..}$)	U$	7.619.304.00
Tunnel cost (C_{tunnel})	U$	177.640.003.50
Powerhouse cost ($C_{p.house}$)	U$	617.992.006.62
Capex cost (C_{Capex})	U$	803.251.314.12
Unit Capex cost (C_{Capex})	U$	1.620.65/kW

Source: author

Table 9
Data for calculating the cost of generated energy (GEC)

FRC	0.1061
Annual Capex Cost ($C_{Anual.Capex}$)	85,208,295.56 U\$/year
Operation and Maintenance cost ($C_{O\&M}$)	40,162,565.71 U\$/year
PSH annual cost ($C_{Annual.\text{PSH}}$)	125,370,861.27 U\$/year
Energy produced annually ($E_{Annual.95}$)	1,137,259.68 MWh/year
Stored Energy Cost ($C_{Energy.\text{Store.}}$)	110.24 U\$/MWh
Cost of solar energy supplied (adopted at auction)	U\$ 35,00
Generated Energy Cost (GEC)	145,24 U\$/MWh

Source: author

the Capex cost was earmarked for operation and maintenance expenses. Equation 18 facilitated the computation of the annual cost of the PSH, providing insights into the ongoing operational expenditure.

Then, the energy stored annually is calculated, considering an availability of 95%, meaning that the system is operational and available for use during 95% of the time for an annual period. And then, as expressed in Equation 19, the cost of the stored energy is calculated. Finally, the cost of the energy generated (GEC) is obtained by Equation 20, synthesizing the findings into a comprehensive framework. Table 9 presents the values used and resulting in the calculations according to the mentioned equations.

This set of procedures provides a comprehensive assessment of the costs associated with PSH implementation. However, due to the fact that some metrics come from the international market, a sensitivity study is carried out to analyze the final cost of the energy generated for different implementation values. Table 10 shows the values obtained for the different percentages of the capital cost. According to the values obtained, it can be said that, for the project in question, it is possible that the energy generated costs between U\$ 112,26/MWh and U\$ 167,22/MWh.

In Mongird *et al.* (2020), a wide range of total implementation cost was estimated, ranging from \$1,349/kW to \$4,048/kW for the PSH, and provided an average cost of \$2,698/kW for a 500 MW plant with 10 hours of generation, in 2010 dollars. Correcting the values to December 2023, according to the CPI Inflation Calculator (USBLS, 2023), a range of \$1,909/kW to \$5,730/kW was obtained, with an average cost of \$3,819/kW.

It is evident that the value obtained for the capital cost (Capex) per kW is lower than that achieved by Mongird *et al.* (2020). This could be attributed to the low cost of storage (related to reservoir construction) in the present study, as this cost is one of the highest in the construction of a PSH. The presence of excavations to act as reservoirs significantly reduces the cost of civil works.

It can be inferred from the results obtained that the selected location is a feasible option for the installation of an PSH, and there are indications that other places may also yield favorable energy outcomes. Solar generation serves as a renewable energy source to be stored by the PSH, yet other renewable sources could also be integrated into the strategy, like wind power. The feasibility study provides a preliminary insight into the installation costs, thereby lending meaning to the actual construction feasibility of the project in the surveyed territory.

5. Conclusion

In this study, an innovative proposal was outlined for the reuse of deactivated mining pits in the Iron Quadrangle, Minas Gerais, transforming them into reservoirs for Reversible Hydroelectric Power Plants (PSH) and providing space for the installation of a Photovoltaic Plant (PVPP).

The results obtained reveal that there is a pair of pits in the established region that meets the necessary requirements for the energy project in question, with considerable potential capable of providing a firm power of 234.27 MW. The cost of energy supplied from the studied project falls within the range between US\$ 112.26/MWh to US\$ 167.22/MWh.

The model of integrating these technologies allowed evaluating their operation over the course of a day. To ensure the self-sufficiency of the project, studies focused on the consistency of solar generation potential coupled with PSH are necessary.

Based on the economic results obtained, it is concluded that the implementation of a PSH in mining-damaged areas will depend on the energy value practiced by the market, but its construction in technological terms is feasible. Implementing this proposal can not only minimize the costs associated with mine closure, attracting investment from private mining sector companies but also contribute to providing energy with lower environmental impact, playing a crucial role in transitioning to a sustainable energy system.

For one of the mines analyzed that is currently in operation, this becomes an alternative for the future when it enters the deactivation phase. The same can be said regarding active mines that were not analyzed for this work, potentially having pit reserves beyond those studied.

As future research, an analysis of the available water source for reservoir replenishment is suggested, given its importance for the execution of the presented project. A detailed evaluation of the PVPP sizing associated is necessary due to its magnitude, as well as further studies aimed at better economic evaluation conditions for implementing this technology. Additionally, a Life Cycle Assessment (LCA) is recommended to assess the environmental performance of the project. These more in-depth analyses can provide valuable insight to guide the successful

Table 10
Sensitivity analysis for the cost

Percentage	70%	80%	90%	100%	110%	120%
Cost of Capital Capex (in 10^6) [U\$]	U\$ 562,28	U\$ 642,60	U\$ 722,93	U\$ 803,25	U\$ 883,58	U\$ 963,90
Unit Capital Cost [U\$/kW]	U\$ 1134,45	U\$ 1296,52	U\$ 1458,58	U\$ 1620,65	U\$ 1782,71	U\$ 1944,78
Operation and Maintenance Cost (in 10^6)	U\$ 40,16					
Annual Capex Cost [U\$/year] (in 10^6)	U\$ 59,65	U\$ 68,17	U\$ 76,69	U\$ 85,21	U\$ 93,73	U\$ 102,25
PSH Annual Cost [U\$/year] (in 10^6)	U\$ 99,81	U\$ 108,33	U\$ 116,85	U\$ 125,37	U\$ 133,89	U\$ 142,41
Stored Energy Cost [U\$/MWh]	U\$ 87,76	U\$ 95,25	U\$ 102,75	U\$ 110,24	U\$ 117,73	U\$ 125,22
Cost of solar energy supplied (adopted at auction) [U\$/MWh]	U\$ 24,50	U\$ 28,00	U\$ 31,50	U\$ 35,00	U\$ 38,50	U\$ 42,00
Generated Energy Cost [U\$/MWh]	U\$ 112,26	U\$ 123,25	U\$ 134,25	U\$ 145,24	U\$ 156,23	U\$ 167,22

Source: author

realization of this proposal, demonstrating that the interaction between environmental sustainability and energy innovation can go hand in hand.

Acknowledgments

The authors would like to thank CNPq – PQ license number: 304370/2018-5/305059/2022-0; Fapemig – license number PPM-00252-18; SEFAC/ANEEL – license number PD-06899-2912/2016 and the Coordination for the Improvement of Higher Education Personnel—Brazil (CAPES).

Author Contributions: AABG: Conceptualization, methodology, formal analysis, writing—original draft, ASB: review and editing, EMFV; supervision, resources, review; VFM: validation and writing—review; CBM: conceptualization, methodology, formal analysis, writing—review and validation.

Funding: This study was financed in part by the Coordenação de Aperfeiçoamento de Pessoal de Nível Superior – Brasil (CAPES) – Finance Code 001.

Conflicts of Interest: The authors declare no conflict of interest.

References

ANM. (2023). *Anuário Mineral Brasileiro Principais Substâncias Metálicas*. www.anm.gov.br

Arnaoutakis, G. E., Kefala, G., Dakanali, E., & Katsaprakakis, D. Al. (2022). Combined Operation of Wind-Pumped Hydro Storage Plant with a Concentrating Solar Power Plant for Insular Systems: A Case Study for the Island of Rhodes. *Energies*, *15*(18). https://doi.org/10.3390/en15186822

Barnes, F. S., & Levine, J. G. (2011). *Large Energy Storage System Handbook* (1st ed.). CRC Press. https://doi.org/10.1201/b10778

Brandão, R., Castro, N. De, & Hunt, J. (2021). *A Viabilidade das Usinas Reversíveis no Sistema Interligado Nacional* (1st ed.). E-Papers.

Canales, F. A., Beluco, A., & Mendes, C. A. B. (2015). *Usinas hidrelétricas reversíveis no Brasil e no mundo: aplicação e perspectivas*. https://doi.org/05902/2236117016002

Cazzaniga, R., Rosa-Clot, M., Rosa-Clot, P., & Tina, G. M. (2019). Integration of PV floating with hydroelectric power plants. In *Heliyon* (Vol. 5, Issue 6). Elsevier Ltd. https://doi.org/10.1016/j.heliyon.2019.e01918

Costa, P. P. N. (2022). *Centrais fotovoltaicas consorciadas à centrais geradoras hidrelétricas (CGHS) – Um estudo de caso* [MSc Dissertation, Universidade Federal de Minas Gerais]. http://hdl.handle.net/1843/47200

CRESESB. (2018). *Potencial Solar - SunData v 3.0.* http://www.cresesb.cepel.br/index.php?section=sundata

Deane, J. P., Ó Gallachóir, B. P., & McKeogh, E. J. (2010). Techno-economic review of existing and new pumped hydro energy storage plant. In *Renewable and Sustainable Energy Reviews*, 14(4),1293–1302). https://doi.org/10.1016/j.rser.2009.11.015

Elera Renováveis. (2023). *Complexo Solar Janaúba*. https://www.elera.com/nossos-ativos/janauba/

EPE. (2019). *Estudos de inventário de usinas hidrelétricas reversíveis*. https://www.epe.gov.br/pt/publicacoes-dados-abertos/publicacoes/nt-006-2019-estudos-de-inventario-de-usinas-hidreletricas-reversiveis

EPE. (2021). *Usinas Hidrelétricas Reversíveis (UHR): Desafios para inserção em mercados de energia elétrica*. http://www.epe.gov.br

EPE. (2022). *LEILÃO DE ENERGIA NOVA A-5 DE 2022*. https://www.epe.gov.br/sites-pt/publicacoes-dados-abertos/publicacoes/PublicacoesArquivos/publicacao-665/Informe%20Vencedores%20LEN%20A5_2022.pdf

FEAM. (2022). *II Cadastro de Minas Paralisadas e Abandonadas do Estado de Minas Gerais*.

Fernandes, P. R. M., & Lima, H. M. de. (2021). O quadro normativo do fechamento de mina e a gestão de minas abandonadas no Brasil e no Estado de Minas Gerais. *Revista Brasileira de Gestão Ambiental e Sustentabilidade*, *8*(18), 352–370. https://doi.org/10.21438/rbgas(2021)081823

Ferreira, T. V. B., Almeida, E. M. de, Mattos, A. D. M. de, Sodré, F. N. A., Salgado, G. de P., Vieira, H. de M., & Conde, M. R. (2022). *Emissão de gases de efeito estufa em Reservatórios Hidrelétricos - NT EPE-DEA-SMA 012/2022.* https://www.epe.gov.br/sites-pt/publicacoes-dados-abertos/publicacoes/PublicacoesArquivos/publicacao-673/NT%20EPE-SMA-DEA_012-2022.pdf

Gol, A. E., & Ščasný, M. (2023). Techno-economic analysis of fixed versus sun-tracking solar panels. *International Journal of Renewable Energy Development*, *12*(3), 615–626. https://doi.org/10.14710/ijred.2023.50165

Görtz, J., Aouad, M., Wieprecht, S., & Terheiden, K. (2022). Assessment of pumped hydropower energy storage potential along rivers and shorelines. *Renewable and Sustainable Energy Reviews*, *165*. https://doi.org/10.1016/j.rser.2021.112027

Guittet, M., Capezzali, M., Gaudard, L., Romerio, F., Vuille, F., & Avellan, F. (2016). Study of the drivers and asset management of pumped-storage power plants historical and geographical perspective. *Energy*, 111, 560–579. https://doi.org/10.1016/j.energy.2016.04.052

Hunt, J. D., Freitas, M. A. V, & Pereira, A. O. (2014). Enhanced-Pumped-Storage: Combining pumped-storage in a yearly storage cycle with dams in cascade in Brazil. *Energy*, *78*, 513–523. https://doi.org/https://doi.org/10.1016/j.energy.2014.10.038

IEA. (2022). World Energy Outlook 2022. www.iea.org/t&c/

IHA. (2022). *Hydropower Status Report*. https://www.hydropower.org/publications/2022-hydropower-status-report

Joseph, A., & Chelliah, T. R. (2018). A review of power electronic converters for variable speed pumped storage plants: Configurations, operational challenges, and future scopes. In *IEEE Journal of Emerging and Selected Topics in Power Electronics* 6(1), 103–119). Institute of Electrical and Electronics Engineers Inc. https://doi.org/10.1109/JESTPE.2017.2707397

Leite, C. R. (2020). *Perda de capacidade de geração em centrais hidrelétricas por efeito da evolução temporal da rugosidade do circuito hidráulico da instalação* [MSc Dissertation]. Universidade Federal de Itajubá.

Libanori, G. H. D., Pinheiro, V. de C. N., & Francato, A. L. (2018). Hybrid power plants as an alternative to fit pumped-storage hydro in Brazilian electricity sector regulatory framework. *International Journal of Energy Research*, *42*(15), 4898–4908. https://doi.org/10.1002/er.4224

Ma, T., Yang, H., Lu, L., & Peng, J. (2015). Pumped storage-based standalone photovoltaic power generation system: Modeling and techno-economic optimization. *Applied Energy*, *137*, 649–659. https://doi.org/https://doi.org/10.1016/j.apenergy.2014.06.005

Margeta, J., & Glasnovic, Z. (2010). Feasibility of the green energy production by hybrid solar + hydro power system in Europe and similar climate areas. In *Renewable and Sustainable Energy Reviews*,14(6),1580–1590). https://doi.org/10.1016/j.rser.2010.01.019

Margeta, J., & Glasnovic, Z. (2012). Theoretical settings of photovoltaic-hydro energy system for sustainable energy production. *Solar Energy*, *86*(3), 972–982. https://doi.org/10.1016/j.solener.2012.01.007

Mongird, K., Viswanathan, V., Alam, J., Vartanian, C., Sprenkle, V., & Baxter, R. (2020). *2020 Grid Energy Storage Technology Cost and Performance Assessment.*

Nibbi, L., Sospiro, P., De Lucia, M., & Wu, C. C. (2022). Improving Pumped Hydro Storage Flexibility in China: Scenarios for Advanced Solutions Adoption and Policy Recommendations †. *Energies*, *15*(21). https://doi.org/10.3390/en15217918

Nikolaos, P. C., Marios, F., & Dimitris, K. (2023). A Review of Pumped Hydro Storage Systems. In *Energies* (Vol. 16, Issue 11). MDPI. https://doi.org/10.3390/en16114516

Oliveira Júnior, J. B. de. (2001). Desativação de empreendimentos mineiros: estratégias para diminuir o passivo ambiental [PhD Thesis, Universidade de São Paulo]. In *Escola Politécnica, Universidade de São Paulo*.

https://www.teses.usp.br/teses/disponiveis/3/3134/tde-22102003-153601/pt-br.php

Rehman, S., Al-Hadhrami, L. M., & Alam, M. M. (2015). Pumped hydro energy storage system: A technological review. In *Renewable and Sustainable Energy Reviews* (Vol. 44, pp. 586–598). Elsevier Ltd. https://doi.org/10.1016/j.rser.2014.12.040

Saigustia, C., & Robak, S. (2021). Review of potential energy storage in abandoned mines in Poland. *Energies* 14(19). MDPI. https://doi.org/10.3390/en14196272

Schreiber, G. P. (1978). *Usinas Hidrelétricas* (1st ed.). Editora Edgard Blucher Ltda.

SEMAD, S. de E. de M.-A. e D. S. (2023). *Deliberação Normativa Copam nº 220, de 21 de março de 2018*. Https://Transparencia.Meioambiente.Mg.Gov.Br/Views/Introducao_fechamento_mina.Php.

Silva, S. B., Severino, M. M., & De Oliveira, M. A. G. (2013). A stand-alone hybrid photovoltaic, fuel cell and battery system: A case study of Tocantins, Brazil. *Renewable Energy*, *57*, 384–389. https://doi.org/10.1016/j.renene.2013.02.004

Silvério, N. M., Barros, R. M., Tiago Filho, G. L., Redón-Santafé, M., Santos, I. F. S. dos, & Valério, V. E. de M. (2018). Use of floating PV plants for coordinated operation with hydropower plants: Case study of the hydroelectric plants of the São Francisco River basin. *Energy Conversion and Management*, *171*, 339–349. https://doi.org/10.1016/j.enconman.2018.05.095

Stocks, M., Stocks, R., Lu, B., Cheng, C., & Blakers, A. (2021). Global Atlas of Closed-Loop Pumped Hydro Energy Storage. *Joule*, *5*(1), 270–284. https://doi.org/10.1016/j.joule.2020.11.015

System Advisor Model (SAM) (2023). https://sam.nrel.gov/download.html

Tonidandel, R. de P. (2011). *Aspectos Legais e Ambientais do Fechamento de Mina no Estado de Minas* [MSc Dissertation, Universidade Federal de Minas Gerais]. https://repositorio.ufmg.br/bitstream/1843/MPBB-8LMGN5/1/rodrigo_tonidandel.pdf

USBLS, B. O. L. S. (2023). *CPI Inflation Calculator*. www.bls.gov

Vilanova, M. R. N., Flores, A. T., & Balestieri, J. A. P. (2020). Pumped hydro storage plants: a review. In *Journal of the Brazilian Society of Mechanical Sciences and Engineering* (Vol. 42, Issue 8). Springer. https://doi.org/10.1007/s40430-020-02505-0

Zakeri, B., & Syri, S. (2015). Electrical energy storage systems: A comparative life cycle cost analysis. In *Renewable and Sustainable Energy Reviews*, 42, 569–596 https://doi.org/10.1016/j.rser.2014.10.011